

Sparse Brains are Also Adaptive Brains: Cognitive-Load-Aware Dynamic Activation for LLMs

Yiheng Yang¹, Yujie Wang^{2*},
Chi Ma², Lei Yu², Emmanuele Chersoni¹, Chu-Ren Huang¹,
¹The Hong Kong Polytechnic University, ²Meituan,

Abstract

Dense large language models (LLMs) face critical efficiency bottlenecks as they rigidly activate all parameters regardless of input complexity. While existing sparsity methods (static pruning or dynamic activation) address this partially, they either lack adaptivity to contextual or model structural demands or incur prohibitive computational overhead. Inspired by human brain’s dual-process mechanisms - predictive coding (N400) for backbone sparsity and structural reanalysis (P600) for complex context - we propose CLADA, a *Cognitive-Load-Aware Dynamic Activation* framework that synergizes statistical sparsity with semantic adaptability. Our key insight is that LLM activations exhibit two complementary patterns: 1) *Global statistical sparsity* driven by sequence-level prefix information, and 2) *Local semantic adaptability* modulated by cognitive load metrics (e.g., surprisal and entropy). CLADA employs a hierarchical thresholding strategy: a baseline from offline error-controlled optimization ensures 40%+ sparsity, dynamically adjusted by real-time cognitive signals. Evaluations across six mainstream LLMs and nine benchmarks demonstrate that CLADA achieves **20% average speedup with <2% accuracy drop**, outperforming Griffin (5%+ degradation) and TT (negligible speedup). Crucially, we establish the first formal connection between neurolinguistic event-related potential (ERP) components and LLM efficiency mechanisms through multi-level regression analysis ($R^2 = 0.17$ for sparsity-adaptation synergy). Requiring no re-training or architectural changes, CLADA offers a deployable solution for resource-aware LLM inference while advancing biologically-inspired AI design. Our code is available at [CLADA](#).

1 Introduction & Related Work

Large Language Models (LLMs) have revolutionized natural language processing through their un-

	MMLU \uparrow	TruthfulQA \uparrow	Winogrande \uparrow	GSM8K \uparrow
LLaMA2-7B	45.83	61.04	74.11	13.95
DejaVu	27.02	51.12	50.2	7.22
TT	45.62	60.66	73.88	13.65
Griffin	43.59	59.26	73.21	12.31
CLADA	44.83	60.45	73.53	13.18

Table 1: Accuracy on benchmarks. Higher values are better. CLADA achieves competitive results on all benchmarks, closely rivaling the baseline LLaMA2-7B.

precedented scale and emergent capabilities. Architectures like LLaMA (Touvron et al., 2023a,b; Grattafiori et al., 2024), Mistral (Jiang et al., 2023), and OPT (Zhang et al., 2022a) demonstrate remarkable in-context learning abilities that scale with parameter count. However, this performance comes at a steep computational cost: modern LLMs require activating billions of parameters per token during inference, creating critical latency bottlenecks (Frantar and Alistarh, 2023). While existing sparsity-based optimization methods attempt to address this challenge through static pruning (Frantar and Alistarh, 2023; Sun et al., 2024; Ashkboos et al., 2024) or mixture-of-experts architectures (Zhang et al., 2022b; Zhu et al., 2024; Szatkowski et al., 2024; Zheng et al., 2024; Pan et al., 2024; Zhong et al., 2024), they fundamentally lack the dynamic adaptability required for natural language processing. Detailed introduction on more related work can be found at Appendix A.

Furthermore, our analysis reveals three key limitations of current dynamic activation approaches (see Table 1): First, the DejaVu (Liu et al., 2023b) sparsity framework fails to adapt to no-RELU activation requirements. Second, threshold-based dynamic activation techniques like TT (Ma et al., 2024) incur prohibitive computational overhead that negates their theoretical speedup potential. Third, training-free methods such as Griffin (Dong et al., 2024) exhibit significant performance degra-

*wangyujie37@meituan.com

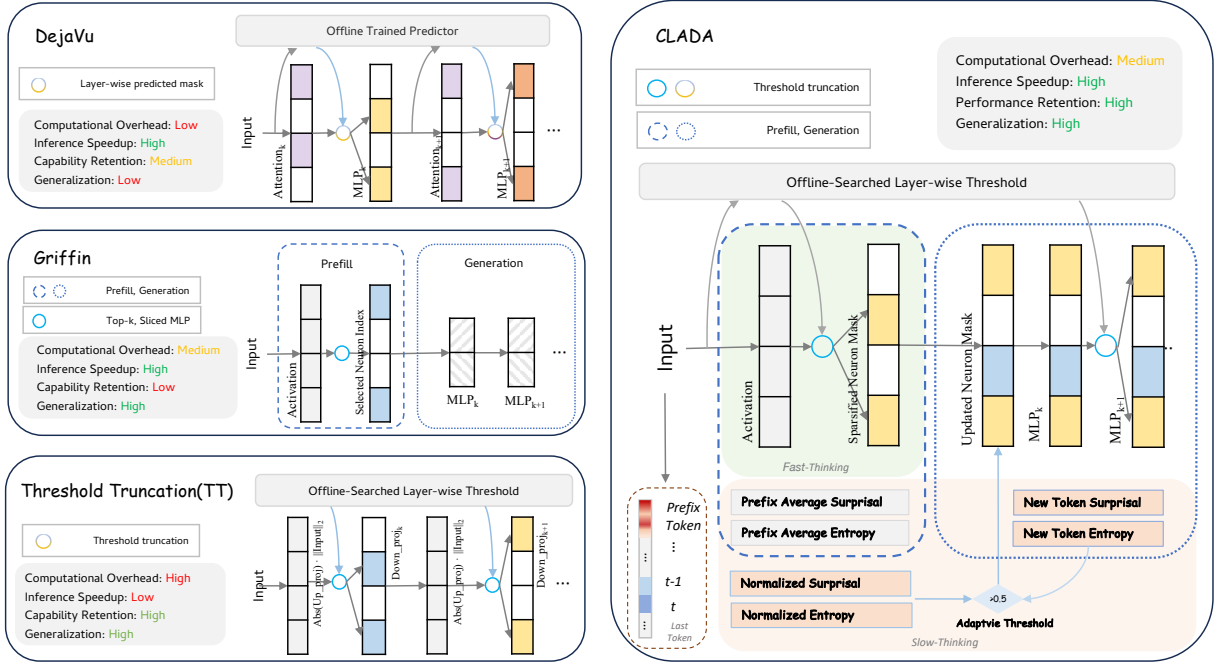


Figure 1: A comparative analysis of dynamic activation methods, highlighting CLADA’s advantages in minimal computational overhead, substantial inference speedup, the ability to maximize model capability, and robust generalization ability across various LLM architectures.

dation (see Table 1) due to their heuristic nature. These shortcomings underscore a fundamental challenge: how to achieve cross-architecture and training-free dynamic computational efficiency while preserving model capacity.

This work draws inspiration from cognitive neuroscience, where the human brain achieves remarkable efficiency through adaptive resource allocation. Neurophysiological studies demonstrate two complementary mechanisms: 1) Predictive coding through the N400 event-related potential (ERP) that minimizes semantic integration costs (Li and Futrell, 2024), and 2) Structural reanalysis via the P600 ERP that handles syntactic complexity (Wilcox et al., 2024). Computational analogs of these mechanisms - surprisal (Hale, 2001; Levy, 2008) and entropy - provide quantitative measures of cognitive load during language processing (Salicchi and Hsu, 2025). The N400-P600 duality in human language processing directly inspires our dual mechanisms: N400-like global sparsity for backbone processing and P600-like local adaptation for complex context.

We posit that LLMs can achieve similar efficiency through two principled sparsity mechanisms:

1. **Statistical Sparsity:** Leveraging sequence-level prefix information to identify and spar-

sify redundant activations;

2. **Semantic Adaptability:** Dynamically allocating computational resources based on real-time cognitive load indicators.

Building on this insight, we propose *Cognitive-Load-Aware Dynamic Activation (CLADA)*, a novel framework that synergizes offline error-controlled optimized threshold truncation with cognitive-load-aware adaptation. Our method introduces three key innovations:

Theoretical Foundation We establish the first connection between cognitive load metrics (surprisal, entropy) and LLM activation patterns, demonstrating their dual role in governing statistical sparsity and semantic adaptation.

Algorithmic Design CLADA introduces a dynamic thresholding mechanism that automatically adjusts activation masks based on both sequence statistics (prefix-based prediction) and semantic complexity (cognitive-load-aware adaptability), requiring no model retraining.

Empirical Validation Extensive experiments across six LLM architectures and nine benchmarks reveal that CLADA achieves 20% average speedup with <2% performance degradation (Table 1 and 5),

while outperforming existing methods in computational overhead and generalization (Table 1).

Our work bridges cognitive science with machine learning, offering a new paradigm for designing efficient yet interpretable language models. By grounding dynamic activation strategies in cognitive theory, we take a significant step toward building LLMs that mirror the adaptive efficiency of biological neural systems.

2 Bridging Cognitive Load and Activation

2.1 Global Statistical Sparsity

Theoretical Framework Statistical sparsity characterizes the phenomenon where neuron activation patterns exhibit hierarchical dependence on sequence prefixes. We formalize this through Hypothesis 2.1:

Hypothesis 2.1 (Existence) *Statistical sparsity manifests as prefix-dependent activation flocking, where activation matrix similarity between hybrid sequences grows monotonically with consistent prefix length.*

This hypothesis aligns with hierarchical representation theories in language modeling (Dubey et al., 2022; Guo et al., 2024), where early tokens establish persistent activation patterns. To operationalize this, we develop a panel regression framework:

$$\Delta_{\text{sim}} = \mu_i + \beta \ell_{ij} + \alpha_i + \epsilon_{ij} \quad (1)$$

where:

- μ_i : Constant term.
- ℓ_{ij} : Prefix length, the subscript j represents data with varying prefix ratios
- α_i : The individual fixed effect term in panel data
- ϵ_{ij} : Random perturbation error term

2.1.1 Experimental Design

Our multi-stage validation framework employs controlled sequence generation and activation pattern analysis:

Corpus Construction Using XSum (Narayan et al., 2018), we create:

- **Natural Language Sequences (NLS)**: 2,000 random authentic text samples

- **Random Token Sequences (RTS)**: 2,000 sequences generated by permuting XSum vocabularies while preserving part-of-speech ratios and punctuation frequency

Hybrid Sequence Generation For each prefix ratio $\alpha \in \{0.25, 0.30, 0.35, 0.40, 0.45, 0.50\}$:

1. Compute prefix length: $\ell = \lceil 2048\alpha \rceil$ ($512 \leq \ell \leq 1024$).
2. Create hybrid sequences A' by replacing first ℓ tokens of NLS-A/RTS-B with NLS-B/RTS-B counterparts.
3. Generate six experimental groups (36,000 sequences in total):
 - NLS-A, NLS-B, NLS-A'
 - RTS-A, RTS-B, RTS-A'

2.1.2 Activation Matrix Extraction

For each sequence, we extract Layer-15 activations from LLaMA-3-8B (Grattafiori et al., 2024) at Token-2049:

$$\mathbf{M}^{(l=15)} \in \mathbb{R}^{1 \times (4096 \times 14336)}$$

The layer selection aligns with previous findings on mid-layer semantic integration (Skean et al., 2025). The rationale for selecting token-2049 is detailed in Appendix B.1.

2.1.3 Similarity Metric Calculation

We compute normalized activation similarity shift:

$$\Delta_{\text{sim}} = \frac{\text{sim}(\mathbf{M}_{A'}, \mathbf{M}_B)}{\text{sim}(\mathbf{M}_A, \mathbf{M}_B)} - 1 \quad (2)$$

where similarity is measured via centered kernel alignment (CKA) (Cortes et al., 2024):

$$\text{sim}_{\text{CKA}}(\mathbf{X}, \mathbf{Y}) = \frac{\|\mathbf{X}^\top \mathbf{Y}\|_F^2}{\|\mathbf{X}^\top \mathbf{X}\|_F \|\mathbf{Y}^\top \mathbf{Y}\|_F} \quad (3)$$

To ensure the robustness of the regression, we additionally employed cosine similarity to quantify the similarity between activation matrices:

$$\text{sim}_{\text{cosine}}(\mathbf{X}, \mathbf{Y}) = \frac{\mathbf{X}^\top \mathbf{Y}}{\|\mathbf{X}\|_2 \|\mathbf{Y}\|_2} \quad (4)$$

Algorithm 1 Empirical Validation of the Existence of Statistical Sparsity

Require: Sequences A, B ; Prefix ratio α

- 1: $A' \leftarrow \text{generate_hybrid_sequence}(A, B, \alpha)$
- 2: $M_A \leftarrow \text{extract_activations}(A)$
- 3: $M_B \leftarrow \text{extract_activations}(B)$
- 4: $M_{A'} \leftarrow \text{extract_activations}(A')$
- 5: $\text{sim}_{AB} \leftarrow \text{sim}(M_A, M_B)$
- 6: $\text{sim}_{A'B} \leftarrow \text{sim}(M_{A'}, M_B)$
- 7: **return** $\Delta_{\text{sim}} = \frac{\text{sim}(M_{A'}, M_B)}{\text{sim}(M_A, M_B)} - 1$

	Dependent variable: $\Delta_{\text{CKA_sim}}$					
	(1) RTS-A'	(2) NLS-A'	(3) RTS-A'	(4) NLS-A'	(5) RTS-A'	(6) NLS-A'
Prefix_len	4.12*** (22.03)	3.91*** (20.16)	4.05*** (21.53)	4.03*** (21.37)	3.75*** (19.22)	3.69*** (18.84)
Surprisal			-0.02 (-0.26)	-0.85*** (-8.19)	-0.09 (-0.14)	-0.80*** (-8.13)
Entropy					-0.36 (-4.38)	-0.12*** (-5.87)
Token_len	10.38*** (5.06)	13.90*** (5.06)	10.14*** (5.07)	12.31*** (5.05)	11.23*** (5.07)	11.38*** (5.06)
Obs	12000	12000	12000	12000	12000	12000
Adjusted R ²	0.13	0.12	0.15	0.16	0.17	0.16
Individual FE	YES	YES	YES	YES	YES	YES
Constant	YES	YES	YES	YES	YES	YES

Note: * p<0.1; ** p<0.05; *** p<0.01

Table 2: Regression results on the impact of $prefix_len$ on CKA activation similarity

2.1.4 Empirical Validation

Experiment 1.1: RTS Groups Following Algorithm 1, construct hybrid sequence A' from RTS B according to Section 2.1.1. Activation matrix similarity is computed using Equation 2.

Observation 1: Regression results (Table 2 Column 1) reveal strong prefix-length effects ($\beta = 4.12, p < 0.001$), confirming Hypothesis 2.1. The robustness check with cosine similarity (Table 3) yields consistent outcomes ($\beta = 4.22, p < 0.001$).

Experiment 1.2: NLS Groups Replicate the aforementioned experimental procedures in Experiment 1.1, regression results of NLS groups are reported in the second column of Table 2.

Observation 2: While maintaining statistical significance ($\beta = 3.91, p < 0.001$) (Table 2 Column 2), the attenuated effect size compared to RTS ($\Delta\beta = 5.4\%$) suggests cognitive-load-aware interference in natural language processing. This observation motivates our investigation of semantic adaptability.

2.1.5 Visual Evidence and Case Study

To investigate the existence of Statistical Sparsity in a visual and intuitive way, we extracted randomly

	Dependent variable: $\Delta_{\text{cos_sim}}$					
	(1) RTS-A'	(2) NLS-A'	(3) RTS-A'	(4) NLS-A'	(5) RTS-A'	(6) NLS-A'
Prefix_len	4.22*** (22.12)	3.94*** (20.41)	4.08*** (21.35)	4.03*** (21.15)	3.71*** (19.46)	3.64*** (18.53)
Surprisal			-0.01 (-0.26)	-0.72*** (-7.32)	-0.07 (-0.12)	-0.80*** (-8.14)
Entropy					-0.35 (-4.25)	-0.12*** (-5.85)
Token_len	10.63*** (5.04)	13.35*** (5.07)	10.65*** (5.02)	12.64*** (5.05)	11.75*** (5.06)	11.34*** (5.03)
Obs	12000	12000	12000	12000	12000	12000
Adjusted R ²	0.12	0.12	0.15	0.16	0.17	0.16
Individual FE	YES	YES	YES	YES	YES	YES
Constant	YES	YES	YES	YES	YES	YES

Note: * p<0.1; ** p<0.05; *** p<0.01

Table 3: Robustness Test: Regression results of $prefix_len$ on cosine activation similarity

two entry from XSum dataset as *Natural Language Sequence-A* (NLS-A) and NLS-B, and replaced the first 512 tokens of NLS-A with NLS-B to produce NLS-A'. Details can be seen in Appendix B.2. And a sentence-by-sentence case study can be seen in Appendix B.3

2.2 Local Semantic Adaptability: Cognitive-Load-Aware Response

Theoretical Foundation The NLS-RTS performance gap (4.12 vs 3.91) reveals a critical limitation of pure statistical sparsity: cognitive load disrupts prefix-dependent activation patterns. We formalize this complementary mechanism through Hypothesis 2.2:

Hypothesis 2.2 (Existence) *Semantic adaptability emerges through cognitive-load-modulated activation adjustments, quantified by surprisal(s_t) and entropy(H_t).*

2.2.1 Operationalization

We extend the regression framework to incorporate cognitive load metrics:

$$\Delta_{\text{sim}} = \mu_i + \beta\ell_{ij} + \gamma_1 s_{ijt} + \gamma_2 H_{ijt} + \alpha_i + \epsilon_{ij} \quad (5)$$

Cognitive Load Quantification Following psycholinguistic theory (Hale, 2016; Oh et al., 2024; Salicchi and Hsu, 2025):

$$s_t = -\log P(w_t|w_{<t}) \quad (\text{surprisal}) \quad (6)$$

$$H_t = -\sum_{w \in \mathcal{V}} P(w|w_{<t}) \log P(w|w_{<t}) \quad (\text{entropy}) \quad (7)$$

where:

- w_t : the target token

- $w_{<t}$: the context of target token
- $P(w_t|w_{<t})$: the conditional probability of target word w_t provided by the language model
- \mathcal{V} : the vocabulary of the language model enriched with special token (e.g., EOS)

And the descriptive statistics of our dataset are reported in Table 9 in Appendix B.

2.2.2 Empirical Validation

Experiment 2: Cognitive-Load-Aware Interference Key findings from Table 2 Columns 3-6:

- **RTS**: Non-significant cognitive-load-aware effects ($\gamma_1 = -0.07, \gamma_2 = -0.35, p > 0.1$)
- **NLS**: Significant inverse correlations ($\gamma_1 = -0.80, \gamma_2 = -0.12, p < 0.001$)

This demonstrates semantic adaptability’s domain-specific nature: high surprisal/entropy tokens in NLS activate emergent neurons (ENs), disrupting prefix-driven activation patterns. The robustness analysis (Table 3 Column 3-6) confirms these effects persist across similarity metrics.

3 Methodology

3.1 Unified Framework: cognitive-Load-Aware Mechanism

The interplay between statistical sparsity and semantic adaptability forms a *hierarchical activation mechanism*, where global efficiency is balanced by local precision.

Core Design

$$A_{\text{total}}^{(t)} = \underbrace{A_{\text{base}}^{(t)}}_{\text{Statistical Sparsity}} + \underbrace{\Delta A_{\text{semantic}}^{(t)}}_{\text{Semantic Adaptability}} \quad (8)$$

where:

- **Statistical Sparsity** ($A_{\text{base}}^{(t)}$): Provides a stable, sequence-level efficiency baseline.
- **Semantic Adaptability** ($\Delta A_{\text{semantic}}^{(t)}$): Dynamically adjusts activation intensity to handle high-cognitive-load contexts.

This dual mechanism aligns with the human brain’s dual-system processing: *System 1* (fast, pattern-driven) and *System 2* (slow, context-aware) (Saha et al., 2024).

3.2 Dynamic Threshold Strategy

3.2.1 Neuron Activation Prefilling

For each layer l , compute neuron-wise activation magnitudes during *prefilling* phase:

$$A_j^{(l)} = \left\| \left[\sigma(W_{\text{in},j}^{(l)}x) \odot V_{\text{in},j}^{(l)}x \right] W_{\text{out},j}^{(l)} \right\|_2 \quad (9)$$

$$\forall j \in [1, d_h^{(l)}]$$

where j indexes neurons in layer l ’s hidden dimension $d_h^{(l)}$. $W_{\text{in},j}^{(l)}$ and $V_{\text{in},j}^{(l)}$ denote the j -th row of input projection matrices. $W_{\text{out},j}^{(l)}$ is the j -th column of output projection matrix.

3.2.2 Layer-wise Base Threshold

Determine optimal base thresholds through error-controlled optimization searching:

$$\tau_{\text{base}}^{(l)} = \arg \max_{\epsilon^{(l)}} \epsilon^{(l)}$$

$$\text{s.t. } \mathbb{E}_{\mathbf{x} \sim \mathcal{D}_{\text{val}}} \left[\text{CETT}^{(l)}(\mathbf{x}; \epsilon^{(l)}) \right] \leq 0.2$$

$$\text{where } \text{CETT}^{(l)} = \frac{\left\| \sum_{j \in \mathcal{S}_{\text{cut}}^{(l)}} n_j^{(l)}(\mathbf{x}) \right\|_2}{\left\| \text{MLP}^{(l)}(\mathbf{x}) \right\|_2} \quad (10)$$

$$\mathcal{S}_{\text{cut}}^{(l)} = \left\{ j \mid A_j^{(l)} < \epsilon^{(l)} \right\}$$

3.2.3 Token-aware Threshold Adjustment

Integrate token-level cognitive signals with layer-wise base thresholds in Equation 11 where token-level metrics are computed as Equation 6 and Equation 7.

- $\mathbb{I}(\cdot)$: Indicator function (1 if condition met, 0 otherwise)
- τ_s, τ_H : Universal thresholds across all layers
- $\lambda^{(l)}, \gamma^{(l)}$: Layer-specific scaling coefficients. Here, we choose 0.80 and 0.12 from Table 2

Algorithm Implementation can be found at Algorithm 2.

4 Experiments

4.1 Experimental Setup

Our approach, along with the baseline models, is implemented using the PyTorch framework, and we leverage the Hugging Face Transformers library for model and dataset management. Our experiments are powered by 1 NVIDIA A100 GPUs with 80 GB of memory. Adhering to the methodologies outlined in Section 3, we sequentially applied

$$\tau_{\text{final}}^{(l)}(t) = \tau_{\text{base}}^{(l)} \cdot \left[1 + \lambda^{(l)} \cdot \mathbb{I}(s_t > \tau_s) + \gamma^{(l)} \cdot \mathbb{I}(H_t > \tau_H) \right] \quad (11)$$

Algorithm 2 CLADA Inference

Input: Model θ , prefix $x_{1:T}$, max gen_len N .

Output: Generated sequence $y_{1:N}$.

- 1: **Prefill Phase:**
 - 2: Search $\tau_{\text{base}}^{(l)}$ and fit $\lambda^{(l)}, \gamma^{(l)}$ for each layer l .
 - 3: Generate initial activation masks $\{\text{Mask}^{(l)}\}$ using $\tau_{\text{base}}^{(l)}$.
 - 4: **Generation Phase:**
 - 5: **for** $t = 1$ to N **do**
 - 6: Compute $s(w_{<T}^{t-1})$ and $H(w_{<T}^{t-1})$.
 - 7: Update thresholds: $\tau_{\text{final}}^{(l)}(t)$
 - 8: Regenerate masks $\{\text{Mask}^{(l)}\}$ by thresholding A_l .
 - 9: Perform sparse forward pass using $\{\text{Mask}^{(l)}\}$ to predict y_t .
 - 10: Update context: $w_{<T}^t = w_{<T}^{t-1} \cup \{y_t\}$.
 - 11: **end for**
-

our methods for each Transformer layers, which reduces inference latency while preserving model performance. All experiments are conducted in a single phase, without any post-training or fine-tuning stages.

Models In this paper, we conducted a comprehensive series of experiments using the OPT-350M, OPT-2.7B, Gemma-2B, LLaMA-2-7B and LLaMA-3-8B and Mistral-7B models. These models represent a significant advancement in language modeling capabilities, providing a spectrum of scales to meet various computational needs and performance benchmarks.

Tasks and Datasets Following Griffin (Dong et al., 2024), we conduct evaluations on a variety of models across multiple generation and classification tasks. For generation tasks, we focus on XSum(Narayan et al., 2018), CNN/DailyMail(Nallapati et al., 2016), COQA(Reddy et al., 2019), and QASPER(Shaham et al., 2022). For classification tasks, our evaluation includes HellaSwag(Zellers et al., 2019), PIQA(Bisk et al., 2019), COPA(Roemmele et al., 2011), ARC-Challenge(Clark et al., 2018), and BoolQ(Clark et al., 2019). Except for XSum and CNN/DailyMail, our experiments utilize the LM Evaluation Harness(Gao et al., 2023).

Baselines Besides comparing against the original LLM, we also evaluate CLADA in relation to Griffin and TT. Unless specified otherwise, each technique is applied in a layer-wise manner, enhancing scalability even when dealing with exceptionally large models. TT has similar performance with CLADA, therefore we only evaluate its generation phase latency. For DejaVu, we did not consider it as a comparable baseline in subsequent experiments(see Table 1).

Sparsity In our evaluation, we especially focus on the MLP blocks of LLM models, which constitute approximately 67% of the parameters of model’s two main blocks, making them a crucial target for dynamic activation. Griffin and CLADA achieves around 50% of sparsity in total.

4.2 Performance Evaluation

Table 4 delineates the performance differences between the Griffin and CLADA methods across various generation and classification tasks. Metrics such as Accuracy (Acc), Rouge-1, and F1 scores were measured across various datasets.

Our comprehensive evaluation across six model architectures and nine benchmarks reveals three key findings regarding CLADA’s effectiveness:

Consistent Superiority Across Scales. CLADA outperforms Griffin across all model sizes:

- Small(OPT-350M): +1.48% on Hellaswag
- Medium(OPT-2.7B): +1.34% on Piqa
- Larger(LLaMA-3-8B): +1.30% on BoolQ

Task-Agnostic Benefits. The advantages manifest across both discriminative and generative tasks:

- Classification: up to 2% higher accuracy on reasoning-heavy benchmarks(ARC-C, Coqa)
- Generation: up to 2.35% better Rouge-1/F1 on summarization(XSum, CNN)

Scaling Characteristics. The performance gap widens with model capacity. Griffin employs a hard top-k, which may discard some important neurons. In contrast, CLADA uses a cognitive-load-aware thresholds, providing greater adaptability.

Models	Acc					Rouge-1		F1	
	Hellaswag	Piqa	Copa	Arc-c	Boolq	Xsum	Cnn	Coqa	Qasper
OPT-350M	32.06	64.64	72.00	21.33	41.01	12.89	14.82	33.39	3.34
Griffin	30.52	62.46	69.00	20.24	39.71	10.59	13.32	31.89	2.14
CLADA	32.00	64.04	72.00	20.73	40.76	11.23	13.47	32.24	2.45
OPT-2.7B	45.86	73.78	77.00	60.77	66.79	18.43	22.24	64.41	7.85
Griffin	43.76	71.84	76.00	58.21	65.92	17.43	20.74	62.91	6.85
CLADA	45.74	73.18	76.00	58.42	66.19	17.86	21.33	64.05	7.70
Gemma-2B	71.40	77.30	83.00	42.10	69.40	15.69	23.32	72.03	12.46
Griffin	70.03	76.34	82.00	41.19	68.42	14.69	22.18	71.78	11.83
CLADA	70.85	76.21	82.00	41.19	68.21	15.32	22.51	72.45	12.33
LLaMA-2-7B	57.16	78.07	87.00	43.34	77.71	27.15	10.08	77.35	26.31
Griffin	56.66	76.57	85.00	41.84	76.21	26.65	8.58	75.85	25.81
CLADA	56.86	77.67	86.00	42.84	77.51	26.85	9.98	76.95	26.11
LLaMA-3-8B	62.53	81.85	93.00	46.29	80.76	29.62	12.21	82.92	28.86
Griffin	62.03	80.35	91.00	43.79	78.26	27.12	11.71	82.42	27.36
CLADA	62.31	81.40	92.00	45.79	80.39	29.47	11.93	82.57	28.37
Mistral-7B	61.21	80.58	92.00	50.43	83.61	28.67	28.00	80.70	24.56
Griffin	59.71	79.08	92.00	47.43	82.11	27.17	26.50	78.20	22.06
CLADA	59.32	79.21	92.00	49.24	83.14	28.35	27.53	80.55	24.07

Table 4: Generation and classification performance across various model architectures. Higher values are better.

4.3 Efficiency Evaluation

Table 5 provides a comparative analysis of the generation latency for various models on a single NVIDIA A100 GPU, using a batch size of 1 and models implemented in FP16 precision via Hugging Face. Both the prompt length and the generated new token length are set to 1024 (longer context results reported in Table 7, and the sparsity of Griffin and CLADA both set to 50%). The unit of reported numbers in Table 5 is seconds.

The results demonstrate that the CLADA method consistently reduces generation latency compared to the dense configuration across all evaluated models. As shown in Table 5, both Griffin and CLADA offer great speedups, ranging from 18-25%, whereas TT maintains a similar generation latency to dense models.

Overall, above results underscore the efficiency of CLADA in accelerating generation speed without significantly compromising task performance, making it a practical and effective solution for optimizing LLMs.

4.4 Ablation Studies

We conduct systematic ablation studies to quantify the contributions of CLADA’s core components.

All experiments maintain identical hyperparameters and evaluation metrics as the main experiments. Ablation study on larger batch size can be seen in Appendix C.

Component Contribution Analysis Table 6 reveals three key findings through controlled component removal:

- **Statistical Sparsity:** Disabling prefix-based activation patterns (**w/o Stat. Sparsity**) causes 17.6 – 23.7% performance degradation across tasks, while only reducing latency by 1.8 – 3.2%. This demonstrates its critical role in preserving model capacity through sequence-level regularities.
- **Semantic Adaptability:** Removing cognitive-load-aware adjustments (**w/o Sem. Adapt.**) maintains latency parity but reduces accuracy by 2.4 – 3.4%, confirming its necessity for handling high-entropy contexts.
- **Dynamic Thresholding:** Replacing our adaptive thresholds with static Top-P=0.5 (**Top-P Threshold**) leads to 14.7-16.3% performance drops, validating the superiority of our theoretically grounded approach.

Models	Dense	TT	Griffin	CLADA
OPT-2.7B	32.95	33.52	26.96(22.22%↓)	27.77(18.65%↓)
Gemma-2B	30.17	30.16	23.92(26.13%↓)	24.06(25.39%↓)
LLaMA-3-8B	81.31	79.88	63.32(22.13%↓)	64.03(21.25%↓)
Mistral-7B	79.28	76.26	63.26(25.32%↓)	63.94(19.34%↓)

Table 5: Generation phase latency(s).

Variant	Accuracy Retention (%)				Latency (s)	
	HellaSwag	PIQA	ARC-C	XSum	OPT-2.7B	LLaMA-3-8B
CLADA (Full)	99.6	99.5	98.9	99.5	27.8	64.0
w/o Stat. Sparsity	80.4	82.1	78.3	76.3	26.9	63.3
w/o Sem. Adapt.	97.1	97.7	96.5	98.3	26.3	62.8
Top-P Threshold	83.3	85.3	86.5	83.6	26.8	62.9

Table 6: Component ablation study. Accuracy Retention = (Variant Score / Dense Baseline) \times 100. Latency measures total time for generating 1024 tokens. Top-P=0.5 serves as static threshold baseline.

Context Length Scalability Table 7 demonstrates CLADA’s superior scalability to long contexts compared to Griffin. While both methods exhibit latency growth with increasing context length, CLADA achieves 1.57 – 1.91s speedup at 32K context due to better memory access patterns in our dynamic thresholding strategy.

5 Conclusion & Discussion

Our work introduces **Cognitively-Load Aware Dynamic Activation (CLADA)**, a novel framework that unifies statistical sparsity and semantic adaptability for efficient LLM inference. The key findings are as follows:

Theoretical Insights We identify and formalize two complementary properties of LLMs’ activation patterns:

1. **Statistical Sparsity:** Activation patterns are dominated by prefix, providing a global efficiency baseline.
2. **Semantic Adaptability:** High-cognitive-load contexts (e.g., unanticipated terms, complex syntax) trigger dynamic adjustments in activation, preserving local precision.

Inference Gains CLADA combines offline-searched TT thresholds with cognitive-load-aware adjustments, achieving 18-25% speedup with less than 2% performance degradation across six LLMs and nine tasks.

For **Future Directions** and **Broader Impact**, please see Appendix D.

Limitations

Despite its advantages, CLADA has several limitations that warrant further investigation:

Pre-filling Overhead For long prefixes (>2048 tokens), the pre-filling phase accounts for 10-15% of the total inference time, reducing the net speedup in real-time applications.

Hardware Constraints Storing activation masks for large models (e.g., LLaMA-70B) increases GPU memory usage, limiting deployment on resource-constrained devices.

References

- Saleh Ashkboos, Maximilian L. Croci, Marcelo Gennari do Nascimento, Torsten Hoefler, and James Hensman. 2024. [Slicept: Compress large language models by deleting rows and columns](#). *Preprint*, arXiv:2401.15024.
- Yonatan Bisk, Rowan Zellers, Ronan Le Bras, Jianfeng Gao, and Yejin Choi. 2019. [Piqa: Reasoning about physical commonsense in natural language](#). *Preprint*, arXiv:1911.11641.
- Rishi Bommasani, Drew A. Hudson, Ehsan Adeli, Russ Altman, Simran Arora, Sydney von Arx, Michael S. Bernstein, Jeannette Bohg, Antoine Bosselut, Emma Brunskill, Erik Brynjolfsson, Shyamal Buch, Dallas Card, Rodrigo Castellon, Niladri Chatterji, Annie Chen, Kathleen Creel, Jared Quincy Davis, Dora Demszky, Chris Donahue, Moussa Doumbouya, Esin Durmus, Stefano Ermon, John Etchemendy, Kawin Ethayarajh, Li Fei-Fei, Chelsea Finn, Trevor Gale, Lauren Gillespie, Karan Goel, Noah Goodman, Shelby Grossman, Neel Guha, Tatsunori Hashimoto,

Models	Prompt Len	Generation Len	Dense	Griffin	CLADA	Diff to Griffin
LLaMA-3-8B (<i>context_len_limit=8K</i>)	1024	1024	80.16	63.32	65.13	-1.68
	2048	1024	84.34	68.08	68.09	-0.01
	2048	2048	87.92	75.86	76.37	-0.51
	4K	2048	92.08	78.03	77.78	0.25
	8K	2048	96.53	84.00	83.79	0.21
Mistral-7B (<i>context_len_limit=32K</i>)	1024	1024	79.28	63.26	64.94	-1.68
	2048	1024	81.37	67.48	68.03	-0.55
	2048	2048	85.46	75.74	76.15	-0.41
	4K	2048	89.26	77.46	77.41	0.05
	8K	2048	93.43	83.79	83.22	0.57
	16K	2048	97.68	86.41	84.50	1.91
	32K	2048	102.35	91.35	89.78	1.57

Table 7: Long-context efficiency comparison(latency in seconds). CLADA outperforms Griffin by up to 1.9s at maximum context lengths.

Peter Henderson, John Hewitt, Daniel E. Ho, Jenny Hong, Kyle Hsu, Jing Huang, Thomas Icard, Saahil Jain, Dan Jurafsky, Pratyusha Kalluri, Siddharth Karamcheti, Geoff Keeling, Fereshte Khani, Omar Khattab, Pang Wei Koh, Mark Krass, Ranjay Krishna, Rohith Kuditipudi, Ananya Kumar, Faisal Ladhak, Mina Lee, Tony Lee, Jure Leskovec, Isabelle Levent, Xiang Lisa Li, Xuechen Li, Tengyu Ma, Ali Malik, Christopher D. Manning, Suvir Mirchandani, Eric Mitchell, Zanele Munyikwa, Suraj Nair, Avanika Narayan, Deepak Narayanan, Ben Newman, Allen Nie, Juan Carlos Niebles, Hamed Nilforoshan, Julian Nyarko, Giray Ogut, Laurel Orr, Isabel Papadimitriou, Joon Sung Park, Chris Piech, Eva Portelance, Christopher Potts, Aditi Raghunathan, Rob Reich, Hongyu Ren, Frieda Rong, Yusuf Roohani, Camilo Ruiz, Jack Ryan, Christopher Ré, Dorsa Sadigh, Shiori Sagawa, Keshav Santhanam, Andy Shih, Krishnan Srinivasan, Alex Tamkin, Rohan Taori, Armin W. Thomas, Florian Tramèr, Rose E. Wang, William Wang, Bohan Wu, Jiajun Wu, Yuhuai Wu, Sang Michael Xie, Michihiro Yasunaga, Jiaxuan You, Matei Zaharia, Michael Zhang, Tianyi Zhang, Xikun Zhang, Yuhui Zhang, Lucia Zheng, Kaitlyn Zhou, and Percy Liang. 2022. [On the opportunities and risks of foundation models](#). *Preprint*, arXiv:2108.07258.

Christopher Clark, Kenton Lee, Ming-Wei Chang, Tom Kwiatkowski, Michael Collins, and Kristina Toutanova. 2019. [Boolq: Exploring the surprising difficulty of natural yes/no questions](#). *Preprint*, arXiv:1905.10044.

Peter Clark, Isaac Cowhey, Oren Etzioni, Tushar Khot, Ashish Sabharwal, Carissa Schoenick, and Oyvind Tafjord. 2018. [Think you have solved question answering? try arc, the ai2 reasoning challenge](#). *Preprint*, arXiv:1803.05457.

Corinna Cortes, Mehryar Mohri, and Afshin Roshtamzadeh. 2024. [Algorithms for learning ker-](#)

[nels based on centered alignment](#). *Preprint*, arXiv:1203.0550.

Harry Dong, Beidi Chen, and Yuejie Chi. 2024. [Prompt-prompted adaptive structured pruning for efficient llm generation](#). *Preprint*, arXiv:2404.01365.

Shiv Ram Dubey, Satish Kumar Singh, and Bidyut Baran Chaudhuri. 2022. [Activation functions in deep learning: A comprehensive survey and benchmark](#). *Preprint*, arXiv:2109.14545.

Jonathan Frankle and Michael Carbin. 2019. [The lottery ticket hypothesis: Finding sparse, trainable neural networks](#). *Preprint*, arXiv:1803.03635.

Elias Frantar and Dan Alistarh. 2023. [Sparsegpt: Massive language models can be accurately pruned in one-shot](#). *Preprint*, arXiv:2301.00774.

Leo Gao, Jonathan Tow, Baber Abbasi, Stella Biderman, Sid Black, Anthony DiPofi, Charles Foster, Laurence Golding, Jeffrey Hsu, Alain Le Noac’h, Haonan Li, Kyle McDonell, Niklas Muennighoff, Chris Ociepa, Jason Phang, Laria Reynolds, Hailey Schoelkopf, Aviya Skowron, Lintang Sutawika, Eric Tang, Anish Thite, Ben Wang, Kevin Wang, and Andy Zou. 2023. [A framework for few-shot language model evaluation](#).

Aaron Grattafiori, Abhimanyu Dubey, Abhinav Jauhri, Abhinav Pandey, Abhishek Kadian, Ahmad Al-Dahle, Aiesha Letman, Akhil Mathur, Alan Schelten, Alex Vaughan, Amy Yang, Angela Fan, Anirudh Goyal, Anthony Hartshorn, Aobo Yang, Archi Mitra, Archie Sravankumar, Artem Korenev, Arthur Hinsvark, Arun Rao, Aston Zhang, Aurelien Rodriguez, Austen Gregerson, Ava Spataru, Baptiste Roziere, Bethany Biron, Binh Tang, Bobbie Chern, Charlotte Caucheteux, Chaya Nayak, Chloe Bi, Chris Marra, Chris McConnell, Christian Keller, Christophe Touret, Chunyang Wu, Corinne Wong, Cristian Canton Ferrer, Cyrus Nikolaidis, Damien Al-lonsius, Daniel Song, Danielle Pintz, Danny Livshits,

Danny Wyatt, David Esiobu, Dhruv Choudhary, Dhruv Mahajan, Diego Garcia-Olano, Diego Perino, Dieuwke Hupkes, Egor Lakomkin, Ehab AlBadawy, Elina Lobanova, Emily Dinan, Eric Michael Smith, Filip Radenovic, Francisco Guzmán, Frank Zhang, Gabriel Synnaeve, Gabrielle Lee, Georgia Lewis Anderson, Govind Thattai, Graeme Nail, Gregoire Milon, Guan Pang, Guillem Cucurell, Hailey Nguyen, Hannah Korevaar, Hu Xu, Hugo Touvron, Iliyan Zarov, Imanol Arrieta Ibarra, Isabel Kloumann, Ishan Misra, Ivan Evtimov, Jack Zhang, Jade Copet, Jaewon Lee, Jan Geffert, Jana Vranes, Jason Park, Jay Mahadeokar, Jeet Shah, Jelmer van der Linde, Jennifer Billock, Jenny Hong, Jenya Lee, Jeremy Fu, Jianfeng Chi, Jianyu Huang, Jiawen Liu, Jie Wang, Jiecao Yu, Joanna Bitton, Joe Spisak, Jongsoo Park, Joseph Rocca, Joshua Johnstun, Joshua Saxe, Jun-teng Jia, Kalyan Vasuden Alwala, Karthik Prasad, Kartikeya Upasani, Kate Plawiak, Ke Li, Kenneth Heafield, Kevin Stone, Khalid El-Arini, Krithika Iyer, Kshitiz Malik, Kuenley Chiu, Kunal Bhalla, Kushal Lakhota, Lauren Rantala-Yeary, Laurens van der Maaten, Lawrence Chen, Liang Tan, Liz Jenkins, Louis Martin, Lovish Madaan, Lubo Malo, Lukas Blecher, Lukas Landzaat, Luke de Oliveira, Madeline Muzzi, Mahesh Pasupuleti, Mannat Singh, Manohar Paluri, Marcin Kardas, Maria Tsimploukelli, Mathew Oldham, Mathieu Rita, Maya Pavlova, Melanie Kam-badur, Mike Lewis, Min Si, Mitesh Kumar Singh, Mona Hassan, Naman Goyal, Narjes Torabi, Nikolay Bashlykov, Nikolay Bogoychev, Niladri Chatterji, Ning Zhang, Olivier Duchenne, Onur Çelebi, Patrick Alrassy, Pengchuan Zhang, Pengwei Li, Petar Vasic, Peter Weng, Prajjwal Bhargava, Pratik Dubal, Praveen Krishnan, Punit Singh Koura, Puxin Xu, Qing He, Qingxiao Dong, Ragavan Srinivasan, Raj Ganapathy, Ramon Calderer, Ricardo Silveira Cabral, Robert Stojnic, Roberta Raileanu, Rohan Maheswari, Rohit Girdhar, Rohit Patel, Romain Sauvestre, Ronnie Polidoro, Roshan Sumbaly, Ross Taylor, Ruan Silva, Rui Hou, Rui Wang, Saghar Hosseini, Sahana Chennabasappa, Sanjay Singh, Sean Bell, Seohyun Sonia Kim, Sergey Edunov, Shaoliang Nie, Shan Narang, Sharath Rapparth, Sheng Shen, Shengye Wan, Shruti Bhosale, Shun Zhang, Simon Vandenhende, Soumya Batra, Spencer Whitman, Sten Sootla, Stephane Collot, Suchin Gururangan, Sydney Borodinsky, Tamar Herman, Tara Fowler, Tarek Sheasha, Thomas Georgiou, Thomas Scialom, Tobias Speckbacher, Todor Mihaylov, Tong Xiao, Ujjwal Karn, Vedanuj Goswami, Vibhor Gupta, Vignesh Ramanathan, Viktor Kerkez, Vincent Gonguet, Virginie Do, Vish Vogeti, Vitor Albiero, Vladan Petrovic, Weiwei Chu, Wenhan Xiong, Wenyan Fu, Whitney Meers, Xavier Martinet, Xiaodong Wang, Xiaofang Wang, Xiaoqing Ellen Tan, Xide Xia, Xinfeng Xie, Xuchao Jia, Xuwei Wang, Yaelle Goldschlag, Yashesh Gaur, Yasmine Babaei, Yi Wen, Yiwen Song, Yuchen Zhang, Yue Li, Yuning Mao, Zacharie DelPierre Coudert, Zheng Yan, Zhengxing Chen, Zoe Papakipos, Aaditya Singh, Aayushi Srivastava, Abha Jain, Adam Kelsey, Adam Shajnfeld, Adithya Gangidi, Adolfo Victoria, Ahuva Goldstand, Ajay Menon, Ajay Sharma, Alex Boesenber, Alexei

Baevski, Allie Feinstein, Amanda Kallet, Amit Sangani, Amos Teo, Anam Yunus, Andrei Lupu, Andres Alvarado, Andrew Caples, Andrew Gu, Andrew Ho, Andrew Poulton, Andrew Ryan, Ankit Ramchandani, Annie Dong, Annie Franco, Anuj Goyal, Aparajita Saraf, Arkabandhu Chowdhury, Ashley Gabriel, Ashwin Bharambe, Assaf Eisenman, Azadeh Yazdan, Beau James, Ben Maurer, Benjamin Leonhardi, Bernie Huang, Beth Loyd, Beto De Paola, Bhargavi Paranjape, Bing Liu, Bo Wu, Boyu Ni, Braden Hancock, Bram Wasti, Brandon Spence, Brani Stojkovic, Brian Gamido, Britt Montalvo, Carl Parker, Carly Burton, Catalina Mejia, Ce Liu, Changhan Wang, Changkyu Kim, Chao Zhou, Chester Hu, Ching-Hsiang Chu, Chris Cai, Chris Tindal, Christoph Feichtenhofer, Cynthia Gao, Damon Civin, Dana Beaty, Daniel Kreymer, Daniel Li, David Adkins, David Xu, Davide Testuggine, Delia David, Devi Parikh, Diana Liskovich, Didem Foss, DingKang Wang, Duc Le, Dustin Holland, Edward Dowling, Eissa Jamil, Elaine Montgomery, Eleonora Presani, Emily Hahn, Emily Wood, Eric-Tuan Le, Erik Brinkman, Esteban Arcaute, Evan Dunbar, Evan Smothers, Fei Sun, Felix Kreuk, Feng Tian, Filippos Kokkinos, Firat Ozgenel, Francesco Caggioni, Frank Kanayet, Frank Seide, Gabriela Medina Florez, Gabriella Schwarz, Gada Badeer, Georgia Swee, Gil Halpern, Grant Herman, Grigory Sizov, Guangyi, Zhang, Guna Lakshminarayanan, Hakan Inan, Hamid Shojanazeri, Han Zou, Hannah Wang, Hanwen Zha, Haroun Habeeb, Harrison Rudolph, Helen Suk, Henry Aspegren, Hunter Goldman, Hongyuan Zhan, Ibrahim Damlaj, Igor Molybog, Igor Tufanov, Ilias Leontiadis, Irina-Elena Veliche, Itai Gat, Jake Weissman, James Geboski, James Kohli, Janice Lam, Japhet Asher, Jean-Baptiste Gaya, Jeff Marcus, Jeff Tang, Jennifer Chan, Jenny Zhen, Jeremy Reizenstein, Jeremy Teboul, Jessica Zhong, Jian Jin, Jingyi Yang, Joe Cummings, Jon Carvill, Jon Shepard, Jonathan McPhie, Jonathan Torres, Josh Ginsburg, Junjie Wang, Kai Wu, Kam Hou U, Karan Saxena, Kartikay Khandelwal, Katayoun Zand, Kathy Matosich, Kaushik Veeraraghavan, Kelly Michelena, Keqian Li, Kiran Jagadeesh, Kun Huang, Kunal Chawla, Kyle Huang, Lailin Chen, Lakshya Garg, Lavender A, Leandro Silva, Lee Bell, Lei Zhang, Liangpeng Guo, Licheng Yu, Liron Moshkovich, Luca Wehrstedt, Madian Khabsa, Manav Avalani, Manish Bhatt, Martynas Mankus, Matan Hasson, Matthew Lennie, Matthias Reso, Maxim Groshev, Maxim Naumov, Maya Lathi, Meghan Keneally, Miao Liu, Michael L. Seltzer, Michal Valko, Michelle Restrepo, Mihir Patel, Mik Vyatskov, Mikayel Samvelyan, Mike Clark, Mike Macey, Mike Wang, Miguel Jubert Hermoso, Mo Metanat, Mohammad Rastegari, Munish Bansal, Nandhini Santhanam, Natascha Parks, Natasha White, Navyata Bawa, Nayan Singhal, Nick Egebo, Nicolas Usunier, Nikhil Mehta, Nikolay Pavlovich Laptev, Ning Dong, Norman Cheng, Oleg Chernoguz, Olivia Hart, Omkar Salpekar, Ozlem Kalinli, Parkin Kent, Parth Parekh, Paul Saab, Pavan Balaji, Pedro Rittner, Philip Bontrager, Pierre Roux, Piotr Dollar, Polina Zvyagina, Prashant Ratanchandani, Pritish Yuvraj, Qian Liang, Rachad Alao, Rachel

- Rodriguez, Rafi Ayub, Raghotham Murthy, Raghu Nayani, Rahul Mitra, Rangaprabhu Parthasarathy, Raymond Li, Rebekkah Hogan, Robin Battey, Rocky Wang, Russ Howes, Ruty Rinott, Sachin Mehta, Sachin Siby, Sai Jayesh Bondu, Samyak Datta, Sara Chugh, Sara Hunt, Sargun Dhillon, Sasha Sidorov, Satadru Pan, Saurabh Mahajan, Saurabh Verma, Seiji Yamamoto, Sharadh Ramaswamy, Shaun Lindsay, Shaun Lindsay, Sheng Feng, Shenghao Lin, Shengxin Cindy Zha, Shishir Patil, Shiva Shankar, Shuqiang Zhang, Shuqiang Zhang, Sinong Wang, Sneha Agarwal, Soji Sajuyigbe, Soumith Chintala, Stephanie Max, Stephen Chen, Steve Kehoe, Steve Satterfield, Sudarshan Govindaprasad, Sumit Gupta, Summer Deng, Sungmin Cho, Sunny Virk, Suraj Subramanian, Sy Choudhury, Sydney Goldman, Tal Remez, Tamar Glaser, Tamara Best, Thilo Koehler, Thomas Robinson, Tianhe Li, Tianjun Zhang, Tim Matthews, Timothy Chou, Tzook Shaked, Varun Vontimitta, Victoria Ajayi, Victoria Montanez, Vijai Mohan, Vinay Satish Kumar, Vishal Mangla, Vlad Ionescu, Vlad Poenaru, Vlad Tiberiu Mihailescu, Vladimir Ivanov, Wei Li, Wenchen Wang, Wenwen Jiang, Wes Bouaziz, Will Constable, Xiaocheng Tang, Xiaojian Wu, Xiaolan Wang, Xilun Wu, Xinbo Gao, Yaniv Kleinman, Yanjun Chen, Ye Hu, Ye Jia, Ye Qi, Yenda Li, Yilin Zhang, Ying Zhang, Yossi Adi, Youngjin Nam, Yu, Wang, Yu Zhao, Yuchen Hao, Yundi Qian, Yunlu Li, Yuzi He, Zach Rait, Zachary DeVito, Zef Rosnbrick, Zhaoduo Wen, Zhenyu Yang, Zhiwei Zhao, and Zhiyu Ma. 2024. [The llama 3 herd of models](#). *Preprint*, arXiv:2407.21783.
- Zhiyu Guo, Hidetaka Kamigaito, and Taro Watanabe. 2024. [Attention score is not all you need for token importance indicator in kv cache reduction: Value also matters](#). *Preprint*, arXiv:2406.12335.
- John Hale. 2001. [A probabilistic Earley parser as a psycholinguistic model](#). In *Second Meeting of the North American Chapter of the Association for Computational Linguistics*.
- John Hale. 2016. Information-theoretical complexity metrics. *Language and Linguistics Compass*, 10(9):397–412.
- Albert Q. Jiang, Alexandre Sablayrolles, Arthur Mensch, Chris Bamford, Devendra Singh Chaplot, Diego de las Casas, Florian Bressand, Gianna Lengyel, Guillaume Lample, Lucile Saulnier, L  lio Renard Lavaud, Marie-Anne Lachaux, Pierre Stock, Teven Le Scao, Thibaut Lavril, Thomas Wang, Timoth  e Lacroix, and William El Sayed. 2023. [Mistral 7b](#). *Preprint*, arXiv:2310.06825.
- Roger Levy. 2008. [Expectation-based syntactic comprehension](#). *Cognition*, 106(3):1126–1177.
- Jiaxuan Li and Richard Futrell. 2024. [Decomposition of surprisal: Unified computational model of erp components in language processing](#). *Preprint*, arXiv:2409.06803.
- Ziang Liu, Genggeng Zhou, Jeff He, Tobia Marcucci, Li Fei-Fei, Jiajun Wu, and Yunzhu Li. 2023a. [Model-based control with sparse neural dynamics](#). *Preprint*, arXiv:2312.12791.
- Zichang Liu, Jue Wang, Tri Dao, Tianyi Zhou, Binhang Yuan, Zhao Song, Anshumali Shrivastava, Ce Zhang, Yuandong Tian, Christopher Re, and Beidi Chen. 2023b. [Deja vu: Contextual sparsity for efficient llms at inference time](#). *Preprint*, arXiv:2310.17157.
- Chi Ma, Mincong Huang, Chao Wang, Yujie Wang, and Lei Yu. 2024. [Dynamic activation pitfalls in llama models: An empirical study](#). *Preprint*, arXiv:2405.09274.
- Eran Malach, Gilad Yehudai, Shai Shalev-Shwartz, and Ohad Shamir. 2020. [Proving the lottery ticket hypothesis: Pruning is all you need](#). *Preprint*, arXiv:2002.00585.
- Ramesh Nallapati, Bowen Zhou, Cicero Nogueira dos santos, Caglar Gulcehre, and Bing Xiang. 2016. [Abstractive text summarization using sequence-to-sequence rnns and beyond](#). *Preprint*, arXiv:1602.06023.
- Shashi Narayan, Shay B. Cohen, and Mirella Lapata. 2018. [Don’t give me the details, just the summary! topic-aware convolutional neural networks for extreme summarization](#). *Preprint*, arXiv:1808.08745.
- Byung-Doh Oh, Shisen Yue, and William Schuler. 2024. [Frequency explains the inverse correlation of large language models’ size, training data amount, and surprisal’s fit to reading times](#). *Preprint*, arXiv:2402.02255.
- Bowen Pan, Yikang Shen, Haokun Liu, Mayank Mishra, Gaoyuan Zhang, Aude Oliva, Colin Raffel, and Rameswar Panda. 2024. [Dense training, sparse inference: Rethinking training of mixture-of-experts language models](#). *Preprint*, arXiv:2404.05567.
- Siva Reddy, Danqi Chen, and Christopher D. Manning. 2019. [Coqa: A conversational question answering challenge](#). *Preprint*, arXiv:1808.07042.
- M. Roemmele, C. A. Bejan, and A. S. Gordon. 2011. Choice of plausible alternatives: An evaluation of commonsense causal reasoning. In *2011 AAAI Spring Symposium Series*.
- Swarnadeep Saha, Archiki Prasad, Justin Chih-Yao Chen, Peter Hase, Elias Stengel-Eskin, and Mohit Bansal. 2024. [System-1.x: Learning to balance fast and slow planning with language models](#). *Preprint*, arXiv:2407.14414.
- Lavinia Salicchi and Yu-Yin Hsu. 2025. [Not every metric is equal: Cognitive models for predicting n400 and p600 components during reading comprehension](#). In *Proceedings of the 31st International Conference on Computational Linguistics*, pages 3648–3654, Abu Dhabi, UAE. Association for Computational Linguistics.

- Uri Shaham, Elad Segal, Maor Ivgi, Avia Efrat, Ori Yoran, Adi Haviv, Ankit Gupta, Wenhan Xiong, Mor Geva, Jonathan Berant, and Omer Levy. 2022. [Scrolls: Standardized comparison over long language sequences](#). *Preprint*, arXiv:2201.03533.
- Oscar Skean, Md Rifat Arefin, Dan Zhao, Niket Patel, Jalal Naghiyev, Yann LeCun, and Ravid Shwartz-Ziv. 2025. [Layer by layer: Uncovering hidden representations in language models](#). *Preprint*, arXiv:2502.02013.
- Mingjie Sun, Zhuang Liu, Anna Bair, and J. Zico Kolter. 2024. [A simple and effective pruning approach for large language models](#). *Preprint*, arXiv:2306.11695.
- Filip Szatkowski, Bartosz Wójcik, Mikołaj Piórczyński, and Simone Scardapane. 2024. [Exploiting activation sparsity with dense to dynamic-k mixture-of-experts conversion](#). *Preprint*, arXiv:2310.04361.
- Hugo Touvron, Thibaut Lavril, Gautier Izacard, Xavier Martinet, Marie-Anne Lachaux, Timothée Lacroix, Baptiste Rozière, Naman Goyal, Eric Hambro, Faisal Azhar, Aurelien Rodriguez, Armand Joulin, Edouard Grave, and Guillaume Lample. 2023a. [Llama: Open and efficient foundation language models](#). *Preprint*, arXiv:2302.13971.
- Hugo Touvron, Louis Martin, Kevin Stone, Peter Albert, Amjad Almahairi, Yasmine Babaei, Nikolay Bashlykov, Soumya Batra, Prajwal Bhargava, Shruti Bhosale, Dan Bikel, Lukas Blecher, Cristian Canton Ferrer, Moya Chen, Guillem Cucurull, David Esiobu, Jude Fernandes, Jeremy Fu, Wenyin Fu, Brian Fuller, Cynthia Gao, Vedanuj Goswami, Naman Goyal, Anthony Hartshorn, Saghar Hosseini, Rui Hou, Hakan Inan, Marcin Kardas, Viktor Kerkez, Madian Khabsa, Isabel Kloumann, Artem Korenev, Punit Singh Koura, Marie-Anne Lachaux, Thibaut Lavril, Jenya Lee, Diana Liskovich, Yinghai Lu, Yuning Mao, Xavier Martinet, Todor Mihaylov, Pushkar Mishra, Igor Molybog, Yixin Nie, Andrew Poulton, Jeremy Reizenstein, Rashi Rungta, Kalyan Saladi, Alan Schelten, Ruan Silva, Eric Michael Smith, Ranjan Subramanian, Xiaoqing Ellen Tan, Binh Tang, Ross Taylor, Adina Williams, Jian Xiang Kuan, Puxin Xu, Zheng Yan, Iliyan Zarov, Yuchen Zhang, Angela Fan, Melanie Kambadur, Sharan Narang, Aurelien Rodriguez, Robert Stojnic, Sergey Edunov, and Thomas Scialom. 2023b. [Llama 2: Open foundation and fine-tuned chat models](#). *Preprint*, arXiv:2307.09288.
- Ethan Gotlieb Wilcox, Tiago Pimentel, Clara Meister, Ryan Cotterell, and Roger P. Levy. 2024. [Testing the predictions of surprisal theory in 11 languages](#). *Preprint*, arXiv:2307.03667.
- Zhihang Yuan, Yuzhang Shang, Yang Zhou, Zhen Dong, Zhe Zhou, Chenhao Xue, Bingzhe Wu, Zhikai Li, Qingyi Gu, Yong Jae Lee, Yan Yan, Beidi Chen, Guangyu Sun, and Kurt Keutzer. 2024. [Llm inference unveiled: Survey and roofline model insights](#). *Preprint*, arXiv:2402.16363.
- Rowan Zellers, Ari Holtzman, Yonatan Bisk, Ali Farhadi, and Yejin Choi. 2019. [Hellaswag: Can a machine really finish your sentence?](#) *Preprint*, arXiv:1905.07830.
- Susan Zhang, Stephen Roller, Naman Goyal, Mikel Artetxe, Moya Chen, Shuohui Chen, Christopher Dewan, Mona Diab, Xian Li, Xi Victoria Lin, Todor Mihaylov, Myle Ott, Sam Shleifer, Kurt Shuster, Daniel Simig, Punit Singh Koura, Anjali Sridhar, Tianlu Wang, and Luke Zettlemoyer. 2022a. [Opt: Open pre-trained transformer language models](#). *Preprint*, arXiv:2205.01068.
- Zhengyan Zhang, Yankai Lin, Zhiyuan Liu, Peng Li, Maosong Sun, and Jie Zhou. 2022b. [Moefication: Transformer feed-forward layers are mixtures of experts](#). *Preprint*, arXiv:2110.01786.
- Haizhong Zheng, Xiaoyan Bai, Xueshen Liu, Z. Morley Mao, Beidi Chen, Fan Lai, and Atul Prakash. 2024. [Learn to be efficient: Build structured sparsity in large language models](#). *Preprint*, arXiv:2402.06126.
- Zexuan Zhong, Mengzhou Xia, Danqi Chen, and Mike Lewis. 2024. [Lory: Fully differentiable mixture-of-experts for autoregressive language model pre-training](#). *Preprint*, arXiv:2405.03133.
- Tong Zhu, Xiaoye Qu, Daize Dong, Jiacheng Ruan, Jingqi Tong, Conghui He, and Yu Cheng. 2024. [Llama-moe: Building mixture-of-experts from llama with continual pre-training](#). *Preprint*, arXiv:2406.16554.

A Related Work

A.1 The Hint of Sparsity

LLMs often appears excessive activation of neurons during tasks, leading to inefficiency and wasted resources(Bommasani et al., 2022; Yuan et al., 2024). Studies(Liu et al., 2023a) show that dense neural networks often display surplus activation. Treating sparsity as a continuous process can optimize model architecture holistically. The Lottery Hypothesis(Frankle and Carbin, 2019; Malach et al., 2020) highlights pruning techniques to remove unnecessary connections and leverage inherent sparsity.

A.2 Static Sparsity

Early efforts to improve LLM efficiency focused on **static sparsity**, where redundant parameters are permanently removed or compressed.

Weight Pruning Methods like SparseGPT(Frantar and Alistarh, 2023) prune weights based on magnitude criteria, achieving up to 50% sparsity without retraining. However, such approaches ignore input-specific sparsity patterns,

leading to suboptimal performance on dynamic tasks like dialogue generation. Static methods lack adaptability to varying input contexts and often require retraining to recover performance.

A.3 Dynamic Activation

Dynamic activation(DA) methods selectively activate subsets of neurons during inference, offering a balance between efficiency and flexibility. Existing researches on dynamic activation methods can be categorized in Table 8.

Training-Dependent Methods DeJaVu(Liu et al., 2023b) predicts activation sparsity during training by leveraging ReLU’s inherent sparsity. While achieving 20% speedup on OPT-style models, it fails on non-ReLU architectures like LLaMA’s SwiGLU.

MoEfication(Zhang et al., 2022b) dynamically routes inputs to expert subnets, but requires costly expert training and introduces routing overhead. DS-MoE(Pan et al., 2024) introduces a framework that employs dense computation during training and switches to sparse computation during inference. LLaMA-MoE(Zhu et al., 2024) offers a new lightweight method to transform FFNs into MoEs. LTE(Zheng et al., 2024) achieves a superior balance between sparsity and performance by activating fewer neurons and is applicable to models with both ReLU and non-ReLU activation functions. Lory(Zhong et al., 2024) retains the autoregressive properties of language models by adopting a causally segmented routing strategy and a similarity-based data batching method. This enables efficient expert merging operations and promotes specialization among experts in processing similar documents during training sessions.

Training-Free Methods Griffin(Dong et al., 2024) uses sequence-level activation clustering (flocking) to skip redundant computations only in generation phase. Despite its simplicity, Griffin suffers from significant performance drops (>3% on QA tasks) due to heuristic threshold selection.

A.4 Cognitive Load and Language Modeling

Cognitive studies on human language processing provide inspiration for efficient computational models. Understanding how humans process language can lead to the development of more efficient and accurate language models. In this section, we explore the relationship between cognitive load, as measured by ERP components such as N400 and

P600, and language modeling metrics like surprisal and entropy.

Surprisal and Entropy Surprisal, proposed by Hale (2001), is defined as the negative log probability of a word given its context. Surprisal captures the idea that the cognitive effort required to process a word is proportional to its unpredictability in a given context. This theory has been widely used to predict human reading times and has been shown to correlate with N400 amplitudes(Salicchi and Hsu, 2025).

Entropy(Oh et al., 2024), on the other hand, measures the level of uncertainty about the upcoming linguistic input at a given point in a sentence. It is calculated based on the probability distribution of possible words in a context and has been linked to the complexity of language processing.

B Details on Bridging Cognitive Load and Activation

B.1 Why Token-2049?

Selecting token-2049 is imperative for the two reasons: 1) The CLADA method introduced in this paper facilitates inference speedup. Thus, it is crucial to examine the activation of the 2049_{th} or latter token when the prefix length is 2048. 2) While analyzing the 2049_{th} token, as opposed to the (*prefix* + 1)_{th} token, may diminish the precision of observed surprisal and entropy effects, it more accurately adheres to the hypothesis of activation flocking.

B.2 Visual Evidence

We plot the whole sequence activation heat-map of NLS-A/B/A’ separately in Figure 4, Figure 5, and Figure 6.

In these figures, the horizontal axis represents the neuron indices, while the vertical axis represents the token indices.

Figures 4 to 6 demonstrate that substituting the initial 512 tokens of NLS-A with the prefix from NLS-B results in an activation pattern that more closely aligns with that of NLS-B.

B.3 Case Study

The mechanism behind statistical sparsity phenomenon needs detailed investigation. When processed as a sequence, activated neurons consider all tokens, suggesting that statistical sparsity may be due to preceding tokens rather than the current token.

DA Types	Definitions	Examples	Advantages	Current Limitations
Training-Dependent DA	Some leverage a <i>predictor</i> , which is pre-trained using the model’s training data, to dynamically identify essential activation neurons or experts during the model’s forward. (Figure 2)	DejaVu (Liu et al., 2023b), MoEfication(Zhang et al., 2022b)	High Sparsity	Tend to underperform on models with non-ReLU activations(See Table 1)
	Others aim to reduce computational costs by employing multi-stage MoE-style training and introducing efficiency and separability loss penalties.	LTE (Zheng et al., 2024) and D2DMoE (Szatkowski et al., 2024)	High performance	Extra training required
Training-Free DA	Employs pre-searched or pre-defined thresholds or sparsity levels to decide which neurons to retain or discard. Neurons with activation values falling below this bar are eliminated during current forward, thereby reducing computational overhead and latency.(Figure 3)	Griffin(Dong et al., 2024), CLADA(Ours)	Training-free for all model archs	Lower performance

Table 8: Two types of DA methods

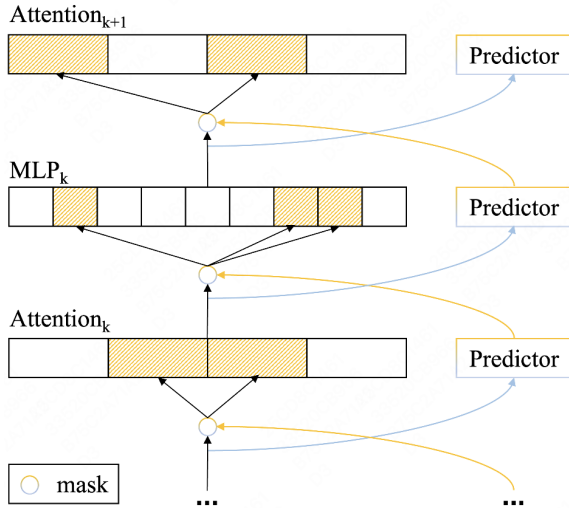


Figure 2: Training-Dependent DA

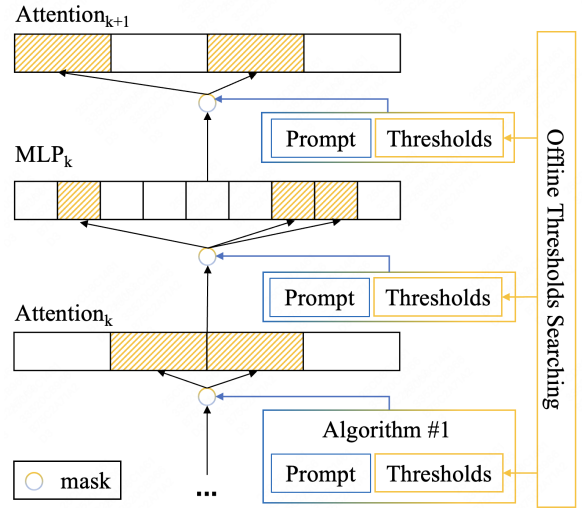


Figure 3: Training-Free DA

	Mean	Std	Min	Max
Prefix_len	-	-	512	1024
Surprisal	0.58	0.31	0.01	1.01
Entropy	0.42	0.45	0.01	1.01
Token_len	2048	0	2048	2048

Table 9: Descriptive statistics of linear regression variables. The *Surprisal* and *Entropy* values in the table are sequence-level normalized to eliminate the impact of inter-sequence variability and absolute magnitude differences.

Batch_size	1	2	4	8	16
Latency	64.03	74.00	76.36	79.33	82.85

Table 10: Batch size scalability analysis. Latency measures total processing time.

To eliminate sequence information influence, we selected specific samples and conducted a similarity analysis of their activation patterns. Details in Table 11 in Appendix B.3.

Table 11 details the 13 samples used for activation pattern similarity analysis. Samples 1-3 and Samples 4, 6, and 9 form two treatment groups. If Sample 4 shows greater similarity to Sample 1 than to Samples 2 and 3, it supports Claim ??.

From the similarity heatmap in Figure 7, we observe the following: a) Samples 4, 6, and 9 are more similarly activated to Sample 1 than to Sam-

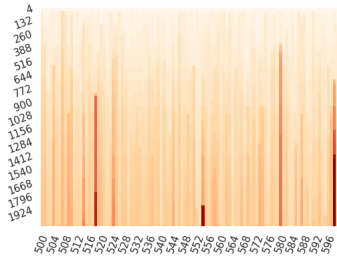


Figure 4: Activation of NLS-A

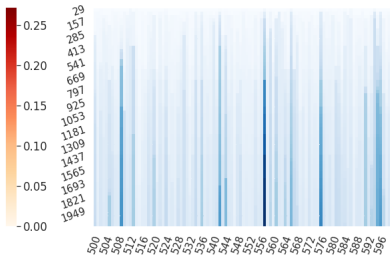


Figure 5: Activation of NLS-B

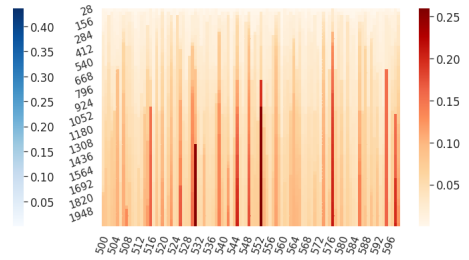


Figure 6: Activation of NLS-A'

ples 2 and 3; b) Samples 1, 6, 8, and 9 are more similarly activated to Sample 4 than to Sample 5; c) Sample 9 is more similarly activated to Samples 4, 6, and 8; d) Samples 11 and 12 are more similarly activated to Samples 9 and 10; e) Samples 10, 11, and 12 are more similarly activated to Sample 13 than to any other samples.

C Batch Size Analysis

We evaluate CLADA’s scalability across different batch sizes using LLaMA-3-8B on XSum summarization. The experiments are conducted on a single NVIDIA A100 GPU with 80GB memory, using FP16 precision. We measure total time for processing the batch. Table 10 indicated that processing time increases sublinearly (27.6% from batch 1 to 16) due to optimized memory access patterns in our dynamic activation strategy.

D More Conclusion

D.1 Future Directions

To address these limitations and extend the impact of CLADA, we propose the following future directions:

1. Cross-Modal Sparsity: Extend CLADA to multimodal models (e.g., LLaVA) by incorporating visual surprisal and entropy metrics for joint text-image processing.
2. Hardware Optimization: Design lightweight mask compression algorithms (e.g., sparse encoding) to reduce memory footprint and enable edge deployment.

D.2 Broader Impact

Beyond efficiency improvements, CLADA offers a new perspective on bridging cognitive science and computational models. By formalizing the connection between cognitive mechanisms and LLM activation patterns, our work paves the way for

more interpretable and biologically plausible AI systems. Furthermore, the training-free nature of CLADA makes it accessible for a wide range of applications, from real-time dialogue systems to on-device language processing.

Index	Samples	Treatments
1	"### Article: Almost one million people visited the city"	Baseline
2	"Article: Almost one million people visited the city"	Remove beginning token
3	"Almost one million people visited the city"	Remove beginning tokens
4	"### Article: Nearly one million people visited the city"	Modify the word at the beginning of the sequence.
5	"Nearly one million people visited the city"	Remove beginning tokens
6	"### Article: Less than one million people visited the city"	Change to antonym
7	"Less than one million people visited the city"	Remove beginning tokens
8	"### Article: Almost one million people visited the city"	Similarity threshold
9	"### Article: Almost one million people visited the restaurant"	Change to synonyms
10	"Almost one million people visited the restaurant"	Modify the word at the end of the sequence
11	"Almost one million people visited the planet"	Modify the word at the end of the sequence
12	"Almost one million tourists visited the restaurant"	Modify the words at the middle and end
13	"Almost one million aliens visited the planet"	Dissimilarity threshold

Table 11: Detailed 13 samples for activation statistical sparsity check.

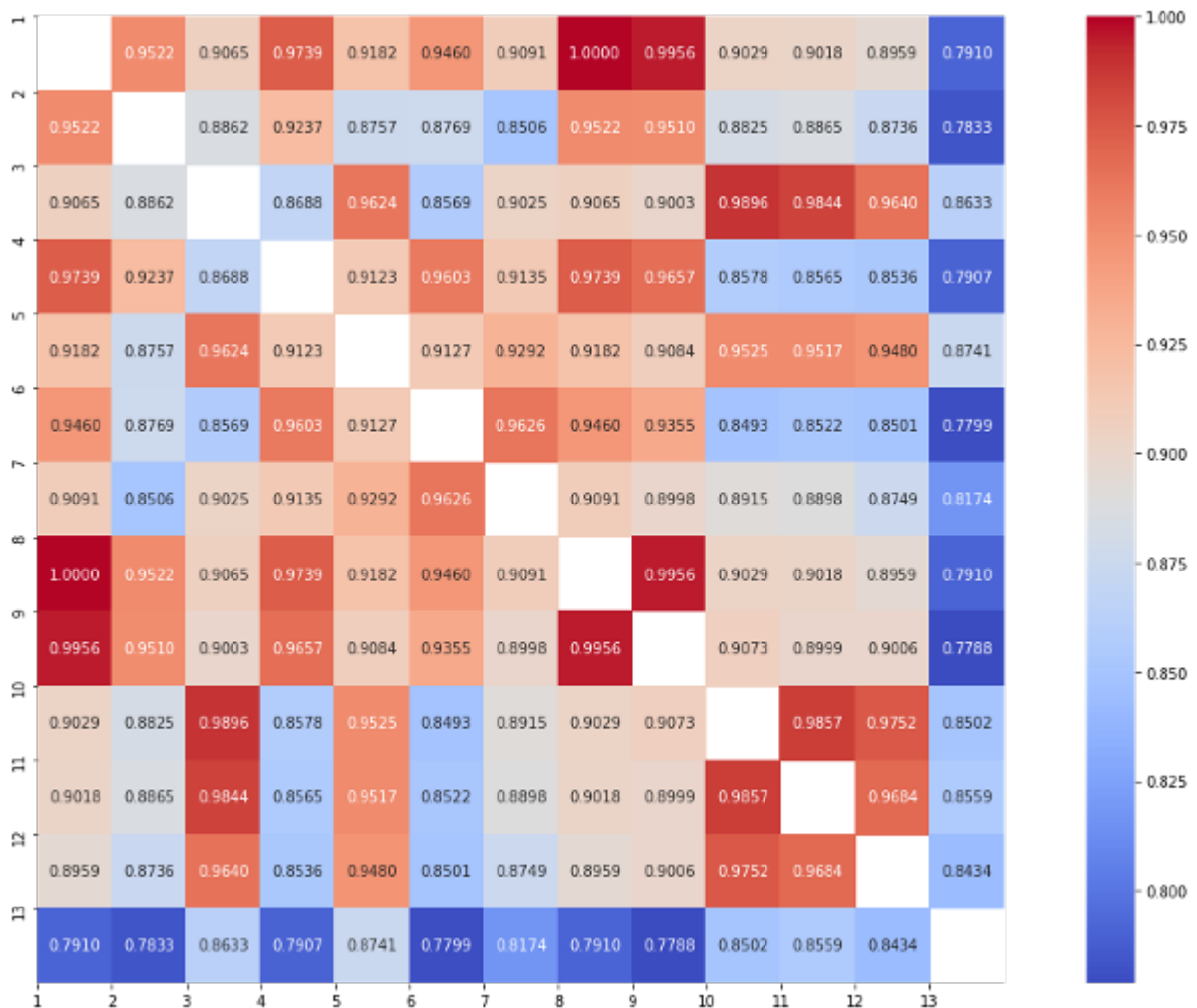


Figure 7: Similarity matrix of 13 samples' activation pattern